Uzbek Journal "Problems of Mechanics"

Research Article

DOI: 10.68846/pmjournal-2026-37-00010

Mathematical model of groundwater head variation processes in heterogeneous porous media

Bakhtiyor Murodullayev[1,2], **Rustam Kodirov**[2*], **Dilobar Haqnazarova**[1]

[1] Digital Technologies and Artificial Intelligence Development Research Institute, 17A, Buz-2, Tashkent, 100125, Uzbekistan
[2] National Institute of Fine Arts and Design named after Kamoliddin Behzod, 123 Mironshokh Street, Tashkent, 100000, Uzbekistan
[3] Tashkent International University of Education, Tuzel-2 Massif, Yashnabad District, Tashkent, 100207, Uzbekistan
[*] **Corresponding author:** qodirov_rr@list.ru

Received: 02 Jule 2026 | **Revised:** 15 August 2026 | **Accepted:** 05 September 2026 | **Published:** 30 September 2026

ABSTRACT

This study develops a mathematical formulation and numerical solution for determining the spatial–temporal distribution of the groundwater head in heterogeneous porous media, and illustrates them with a transient multi-well simulation. The relevance of the study stems from the need for efficient management of groundwater resources, for ecological sustainability, and for forecasting hydrological processes under a changing climate. Starting from Darcy's law and the law of mass conservation, a second-order parabolic partial differential equation with variable coefficients is derived that describes filtration in anisotropic heterogeneous media; anisotropy is represented through a diagonal hydraulic-conductivity tensor and heterogeneity through spatially variable parameters. Boundary conditions are formulated for all six faces of the domain, including river–aquifer interaction, infiltration, evapotranspiration, and irrigation return flow. The differential problem is discretized by an explicit finite-difference scheme in which the interface conductivities in the heterogeneous medium are evaluated by the harmonic mean, which correctly reproduces series-connected hydraulic resistances. The stability of the scheme is analysed by the von Neumann method and a Courant–Friedrichs–Lewy stability condition is obtained; convergence follows from the Lax equivalence theorem. A transient numerical experiment is carried out for a 2000×2000 m aquifer containing two extraction wells and one injection well: the computations reproduce the progressive formation and interaction of the depression cones and the recharge mound, the transient head response at the wells, and the three-dimensional structure of the head surface. The computational algorithm parallelizes naturally and can be applied to groundwater-resource management, to forecasting the hydrodynamic state of aquifers, and to the design of wells and drainage systems.

KEYWORDS

groundwater flow, heterogeneous porous media, finite-difference method, anisotropy, piezometric head, well hydraulics, numerical stability

1. Introduction

Efficient management of groundwater resources and forecasting their future state is one of the central tasks of modern hydrogeology. Its solution requires mathematical models that adequately reproduce the underlying physical processes. In recent years significant progress has been made in the mathematical modeling of groundwater dynamics, particularly in improving numerical methods, discretization schemes, and computational algorithms; the main directions relevant to the present study are reviewed below.

The flexibility of the mesh geometry is of great importance in the numerical solution of the filtration equation in heterogeneous media. A multi-point flux approximation (MPFA) for the conservative form of the diffusion equation on arbitrary polygonal grids provides correct fluxes even when the principal axes of the conductivity tensor are not aligned with the mesh edges, which is a clear advantage for anisotropic heterogeneous media [1]. Meshless techniques avoid grid construction altogether: a hybrid meshless local Petrov–Galerkin method combined with a particle filter, in which the weak-form integrals are evaluated with radial basis functions and parameters are updated through Bayes' theorem, showed reduced error for free-surface aquifer modeling [2]. The generalized finite-difference method (GFDM), which approximates spatial derivatives from a Taylor expansion around an arbitrary node using moving least squares, was applied to a large free-surface aquifer and showed good agreement with MODFLOW [3]. At the regional scale, the finite-volume formulation of MODFLOW 6 on an unstructured quadtree grid was used to build a national-scale, geologically complex, multi-layer model of Great Britain with several hundred thousand active cells [4].

A separate and rapidly growing direction is the use of machine learning. Physics-informed neural networks (PINNs), whose loss function combines a data-misfit term with the residual of the differential equation evaluated by automatic differentiation, have been applied to transient unconfined groundwater flow and perform well even under data scarcity [5]; their mathematical foundations, advantages, and open problems in groundwater modeling have been analysed in detail [6]. Broader reviews summarise the integration of deep learning into hydrogeological modeling [7] and the use of data-driven and surrogate models, including Bayesian networks for uncertainty quantification, for flow and transport in porous media [8]. Among high-order mesh-based methods, control-volume isogeometric analysis with NURBS basis functions yields smooth velocity fields with optimal convergence regardless of the degree of heterogeneity [9], while reduced-order modeling based on proper orthogonal decomposition accelerates repeated groundwater simulations [10]. Regional research groups have also advanced the numerical modeling of multi-phase and multi-layer filtration in deformable and heterogeneous media [11, 12], and recent surveys review the state of the art in groundwater modeling as a whole [13].

Despite this progress, the explicit finite-difference method retains an important role: it rests on the classical foundations of the theory

of groundwater motion [14–16], it is transparent and easy to verify, it handles heterogeneity naturally through conservative interface averaging [17, 18], and it parallelizes almost trivially. The present paper is devoted to the complete formulation of such a model. We derive the governing parabolic equation for the groundwater head in a heterogeneous anisotropic three-dimensional medium, formulate the full set of boundary conditions, construct an explicit conservative finite-difference scheme with a von Neumann stability analysis, and demonstrate the approach on a transient numerical experiment with two extraction wells and one injection well.

2. Problem formulation

The object of study is an aquifer – a water-bearing geological layer occupying a three-dimensional region. The computational domain is taken as a rectangular parallelepiped

$$\Omega = \{(x, y, z) : \ 0 \leqslant x \leqslant L_x, \ 0 \leqslant y \leqslant L_y, \ 0 \leqslant z \leqslant L_z\}, \tag{1}$$

where L_x, L_y, L_z are the dimensions along the axes; x points west–east, y south–north, and z vertically upward. The unknown is the piezometric head $h(x, y, z, t)$, which, following Bernoulli's relation, expresses the specific mechanical energy of a fluid particle per unit weight,

$$h = \frac{p}{\rho g} + z, \tag{2}$$

with p the pore pressure, ρ the density of water and g the gravitational acceleration; fluid moves in the direction of decreasing head [16].

Natural media are generally heterogeneous and anisotropic. The hydraulic conductivity is a symmetric positive-definite second-rank tensor; aligning the axes with the principal directions of anisotropy diagonalises it,

$$\mathbf{K} = diag\left(K_x, K_y, K_z\right), \qquad K_x \approx K_y \gg K_z, \tag{3}$$

the inequality reflecting the layered structure of sedimentary rocks. The specific storage

$$S_s = \rho g \left(\alpha + n\beta\right) \tag{4}$$

characterises the elastic response of the aquifer, where α is the compressibility of the skeleton, n the porosity and β the compressibility of water.

The model rests on two laws. Darcy's law for an anisotropic medium reads, in tensor and component form,

$$\mathbf{q} = -\mathbf{K}\,\nabla h, \qquad q_x = -K_x \frac{\partial h}{\partial x}, \ \ q_y = -K_y \frac{\partial h}{\partial y}, \ \ q_z = -K_z \frac{\partial h}{\partial z}, \tag{5}$$

where $\mathbf{q}$ is the Darcy velocity [14]. Mass conservation in a control volume gives

$$S_s \frac{\partial h}{\partial t} = -\nabla \cdot \mathbf{q} + W, \tag{6}$$

with W the volumetric source/sink intensity. Substituting (5) into (6) yields the governing equation

$$S_s \frac{\partial h}{\partial t} = \frac{\partial}{\partial x}\left(K_x \frac{\partial h}{\partial x}\right) + \frac{\partial}{\partial y}\left(K_y \frac{\partial h}{\partial y}\right) + \frac{\partial}{\partial z}\left(K_z \frac{\partial h}{\partial z}\right) + W, \tag{7}$$

a second-order parabolic equation with variable coefficients. Expanding a diffusion term for a heterogeneous medium,

$$\frac{\partial}{\partial x}\left(K_x \frac{\partial h}{\partial x}\right) = K_x \frac{\partial^2 h}{\partial x^2} + \frac{\partial K_x}{\partial x}\frac{\partial h}{\partial x}, \tag{8}$$

reveals an advective term proportional to ∇K that draws water toward high-conductivity zones.

The source/sink term collects the external influences on the water balance. Wells are modeled as point sources [15, 19],

$$W_{well} = \sum_{i=1}^{N_w} \frac{Q_i}{V_i}\,\delta_i(x, y, z), \tag{9}$$

where Q_i is the discharge of the i-th well (negative for extraction, positive for injection), V_i the volume of its perforated interval and δ_i the location indicator; a cone-shaped depression forms around an extraction well. Vertical exchange through semi-pervious aquitards in multilayer systems is described by a leakage term [20]

$$W_{leak} = \frac{K'}{b'}\left(h_{adj} - h\right), \tag{10}$$

with K'/b' the leakance and h_{adj} the head in the adjacent aquifer; drainage elements are represented analogously through a conductance acting only above the drain elevation.

Boundary conditions are prescribed on each face of Ω. On the lateral boundaries a third-kind (Robin) condition is used, e.g. at $x = 0$,

$$-K_x \left.\frac{\partial h}{\partial x}\right|_{x=0} = \alpha_b \ (h_{ext} - h) + q_{ext}, \tag{11}$$

where α_b is the boundary conductance, h_{ext} the external head and q_{ext} the external flux; where a river borders the domain, the exchange $Q_{riv} = C_r\,(h_r - h)$ is added, and the Dirichlet ($\alpha_b \to \infty$) and no-flow ($\alpha_b \to 0$, $q_{ext} = 0$) conditions are recovered as limits. The base $z = 0$ is treated as impervious (or weakly leaky), and at the land surface $z = L_z$ a flux condition

$$-K_z \frac{\partial h}{\partial z}\bigg|_{z=L_z} = N = I - ET + R \tag{12}$$

collects infiltration I, evapotranspiration ET and irrigation return R. The problem is closed by the initial condition

$$h(x, y, z, 0) = h_0(x, y, z). \tag{13}$$

Real heterogeneity is prescribed either deterministically, e.g. an exponential decay of conductivity with depth $K(z) = K_0 \exp\left[-(L_z - z)/\updownarrow_K\right]$ due to compaction, or stochastically through $\ln K(\mathbf{x}) = \langle lnK\rangle + \sigma_Y Y(\mathbf{x})$ with a standardised random field Y [17]. With these data, and boundary conditions of Robin/Dirichlet/Neumann type, the parabolic problem (7) is well posed in the sense of Hadamard.

3. Numerical method

The differential problem is solved by an explicit conservative finite-difference scheme. A uniform grid $x_i = i\,\Delta x$, $y_j = j\,\Delta y$, $z_k = k\,\Delta z$, $t^n = n\,\Delta t$ is introduced, and h^n_{ijk} denotes the nodal approximation. The time derivative is replaced by a forward difference of order $O(\Delta t)$, and each diffusion term is written in the conservative Patankar form [18], e.g.

$$\frac{\partial}{\partial x}\left(K_x \frac{\partial h}{\partial x}\right)_{ijk} \approx \frac{K_{i+\frac{1}{2},j,k}\left(h_{i+1,j,k} - h_{i,j,k}\right) - K_{i-\frac{1}{2},j,k}\left(h_{i,j,k} - h_{i-1,j,k}\right)}{\Delta x^2}, \tag{14}$$

where the interface conductivities are evaluated by the *harmonic mean*, which reproduces the equivalent resistance of series-connected layers and vanishes next to an impermeable block [17],

$$K_{i+\frac{1}{2},j,k} = \frac{2\,K_{i,j,k}\,K_{i+1,j,k}}{K_{i,j,k} + K_{i+1,j,k}}. \tag{15}$$

Collecting the terms gives the explicit update for interior nodes,

$$h^{n+1}_{ijk} = h^n_{ijk} + \frac{\Delta t}{S_s}\left(\mathcal{D}^n_x + \mathcal{D}^n_y + \mathcal{D}^n_z + W^n_{ijk}\right), \tag{16}$$

in which $\mathcal{D}^n_x, \mathcal{D}^n_y, \mathcal{D}^n_z$ are the interface-conductivity differences (14) along the three axes; the new value is thus an explicit weighted combination of the central node and its six neighbours at the previous time level, and no linear system need be solved. Wells enter W^n_{ijk} through $Q_i/(\Delta x \Delta y \Delta z)$ at the perforated cells (with an equivalent-radius correction [19]); the Robin condition (11) is solved algebraically at boundary nodes and reduces to the Dirichlet or no-flow forms in the corresponding limits.

Being explicit, the scheme is conditionally stable. A von Neumann analysis [21], evaluated at the most restrictive node (largest conductivity, smallest storage), gives the Courant–Friedrichs–Lewy condition

$$\Delta t \leqslant \frac{S_s}{2\left(K_x^{\max}/\Delta x^2 + K_y^{\max}/\Delta y^2 + K_z^{\max}/\Delta z^2\right)}, \tag{17}$$

which is applied with a safety factor $\eta < 1$; by the Lax equivalence theorem [22] consistency together with (17) guarantees convergence of order $O(\Delta t) + O\left(\Delta x^2\right)$. The algorithm is therefore compact: precompute the interface conductivities and check (17); then, at each step, evaluate the sources, update the boundaries, and advance the interior nodes by (16). Since every node depends only on previous-level neighbours, the method maps directly onto OpenMP, MPI, or GPU parallelism; its main limitation is the step restriction (17), which favours implicit schemes only when very long times must be simulated.

4. Numerical experiment and results

The scheme was applied to a transient multi-well problem representative of a confined aquifer under combined extraction and managed recharge. A square horizontal domain of 2000×2000 m was discretized by a uniform 161×161 grid; the transmissivity was $T = Kb = 1.2 \times 10^{-3}$ m^2/s (conductivity $K = 6 \times 10^{-5}$ m/s, thickness $b = 20$ m) and the storativity $S = 3 \times 10^{-3}$. A gentle regional gradient (heads rising from about 43 to 48 m toward the north-east) was imposed as a Dirichlet condition on the outer boundary and as the initial field. Three fully penetrating wells were operated: two extraction wells, W_1 at $(600, 1000)$ m with $Q_1 = -0.027$ m^3/s and W_2 at $(1400, 700)$ m with $Q_2 = -0.011$ m^3/s, and one injection well, W_3 at $(1000, 1600)$ m with $Q_3 = +0.013$ m^3/s. By condition (17) the time step was $\Delta t \approx 88$ s, and the transient was followed for 274 h.

The evolution of the head field is shown in Fig. 1. From the initial regional plane, two depression cones develop around the extraction wells and a recharge mound around the injection well; all three grow with time and progressively distort the regional flow. The cones are not perfectly radial: the contour lines are stretched along the regional gradient and compressed against it, and the strong well W_1 and the weaker W_2 interact, forming a broad low-head corridor between them. The head range widens monotonically, from $[30.0, 53.9]$ m at $t = 9.8$ h to $[24.7, 54.7]$ m at $t = 274.2$ h, showing that the system is still approaching, but has not yet reached, a steady state.

The transient response is quantified in Fig. 2, which tracks the head at each well. All three curves display the characteristic logarithmic, Theis-type behaviour – fast initial change followed by a gradual slow-down as the cone of influence expands. By the end of the simulation the drawdown reaches 20.6 m at the strong well W_1 and 9.1 m at W_2, while the injection well W_3 builds up by 8.2 m; the ratio of the W_1 and W_2 drawdowns is close to the ratio of their discharges, as expected for a confined aquifer in the quasi-linear regime, with the remaining difference explained by well interference and by the position of each well relative to the regional gradient. The monotone, oscillation-free curves also confirm that the step chosen from (17) keeps the explicit scheme stable.

Figure 3 gives an integrated three-dimensional view of the head surface at the final time: the two extraction funnels and the injection peak are clearly resolved against the inclined regional background, and their partial overlap illustrates the superposition of well responses that governs well-field design. Taken together, the three figures show that the explicit conservative scheme reproduces the expected qualitative hydraulics – transient cone growth, well interference, the balancing effect of injection, and the distortion of the flow field by the regional

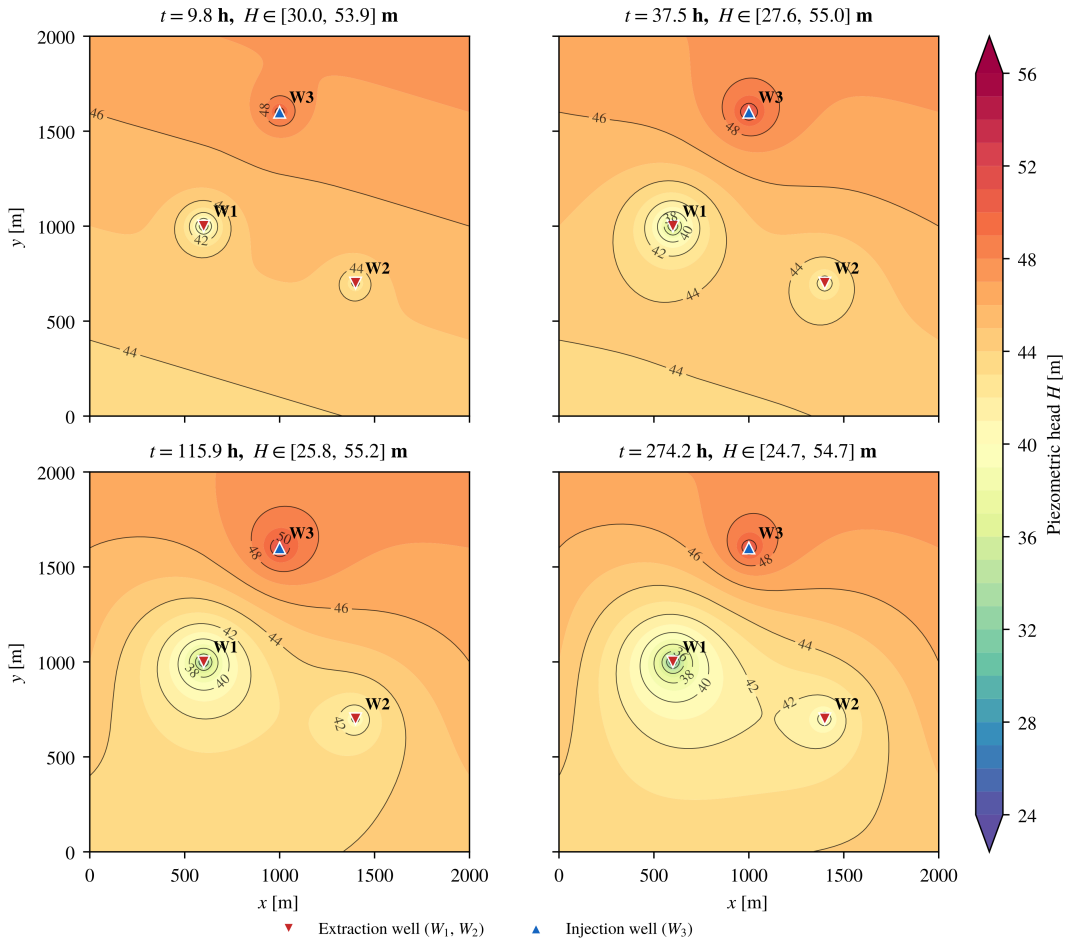


Figure 1. Evolution of the piezometric head $H(x, y)$ at $t = 9.8$, 37.5, 115.9 and 274.2 h. Red triangles are the extraction wells W_1, W_2; the blue triangle is the injection well W_3. The colour scale is common to all four panels.

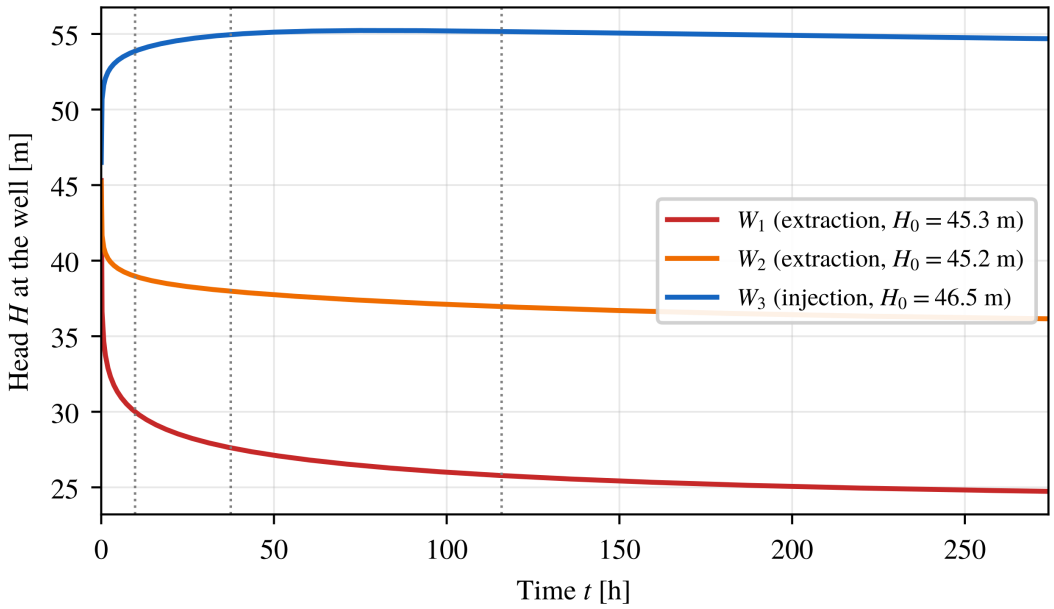


Figure 2. Transient head response at the three wells. The extraction wells W_1, W_2 draw down while the injection well W_3 builds up; dotted lines mark the four snapshot times of Fig. 1.

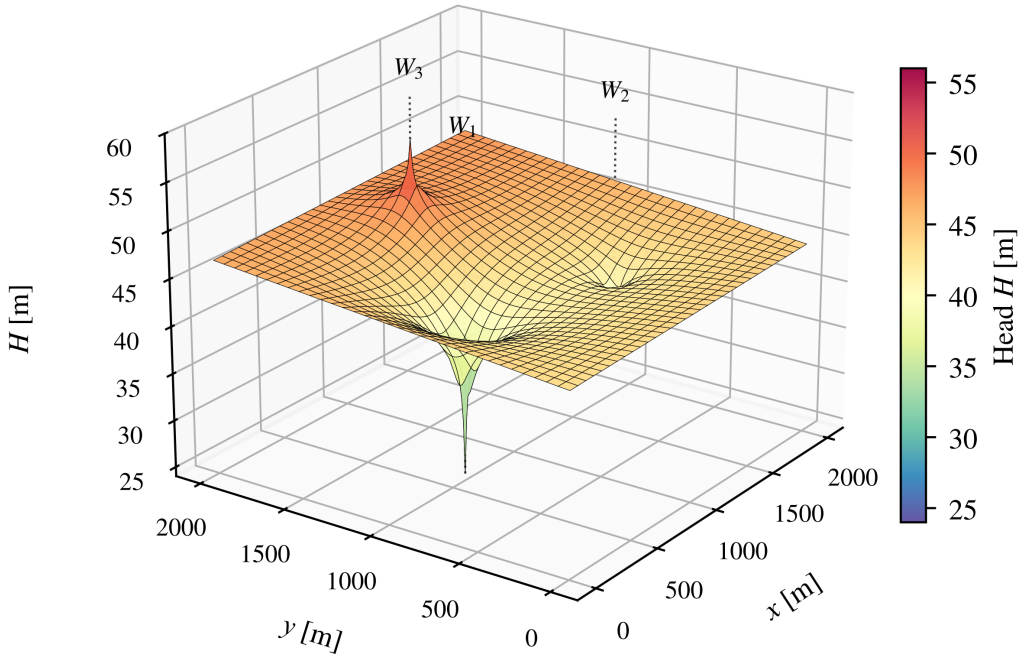


Figure 3. Three-dimensional view of the head surface at $t = 274.2$ h. The two funnels are the extraction cones (W_1, W_2) and the peak is the injection mound (W_3), superimposed on the inclined regional surface.

gradient – while remaining stable and strictly conservative. The results are physically consistent throughout: the head stays bounded between the injection and extraction limits, the depression and recharge zones are centred on the corresponding wells, and the drawdowns scale with the pumping rates. Quantitative verification and validation of the scheme are reported in the next subsection.

5. Verification and validation

Because the qualitative behaviour above is not, by itself, evidence of numerical correctness, the scheme was verified and validated quantitatively. *Validation against an analytical solution.* For a single well of discharge $Q_w = -0.02$ m^3/s in a homogeneous confined aquifer ($T = 1.2\times10^{-3}$ m^2/s, $S = 3\times10^{-3}$), the computed transient drawdown was compared with the Theis solution $s(r,t) = \frac{-Q_w}{4\pi T} W(u)$, $u = \frac{r^2 S}{4Tt}$, where W is the exponential integral. At $t = 6$ h the numerical and analytical drawdowns agree to within 1.6% for $r \gtrsim 3\Delta x$ (Fig. 4a); the larger deviation at the first node adjacent to the well is the expected grid-scale representation of a point source and is reduced by refinement or a well-index correction. *Grid convergence.* Refining the mesh ($\Delta x = 33.3, 16.7, 8.3$ m) makes the drawdown at $r = 100$ m converge monotonically toward the analytical value (Fig. 4b), the change over the last refinement being 0.6%. *Time-step convergence.* Halving the time step from the stability limit changes the same drawdown by less than 0.5%, confirming that the step prescribed by the CFL condition is adequate. *Mass conservation.* Over the transient the water released from storage equals the pumped volume to within 0.5% (pumped 432 m^3 vs. storage release 434 m^3, the small difference being far-field boundary recharge), confirming the global conservation of the conservative scheme.

6. Conclusions

A mathematical model of groundwater head variation in heterogeneous porous media has been developed and demonstrated. A second-order parabolic equation with variable coefficients was derived from Darcy's law and the law of mass conservation, accounting for anisotropy through a diagonal conductivity tensor and for heterogeneity through spatially variable parameters; boundary conditions were formulated for all six faces of the domain, including river–aquifer interaction, infiltration, evapotranspiration and irrigation return, and the problem was shown to be well posed in the sense of Hadamard.

For the numerical solution an explicit conservative finite-difference scheme was constructed, with interface conductivities evaluated by the harmonic mean, which correctly represents series-connected hydraulic resistances. The stability of the scheme was established by a von Neumann analysis and expressed as a Courant–Friedrichs–Lewy condition, and convergence follows from the Lax equivalence theorem. A transient numerical experiment with two extraction wells and one injection well reproduced the progressive formation and interaction of the depression cones and the recharge mound, the Theis-type transient head response at the wells (final drawdowns of 20.6 and 9.1 m and a build-up of 8.2 m), and the three-dimensional structure of the head surface, while remaining stable and mass-conservative.

Because each node is updated independently of the others at every step, the algorithm parallelizes naturally on multi-core and GPU architectures. The model and the method can be applied to groundwater-resource management, to forecasting the hydrodynamic state of aquifers, and to the design of wells and drainage systems; natural extensions include heterogeneous stochastic conductivity fields, coupling with solute transport, and a comparison with implicit schemes for long-term simulation.

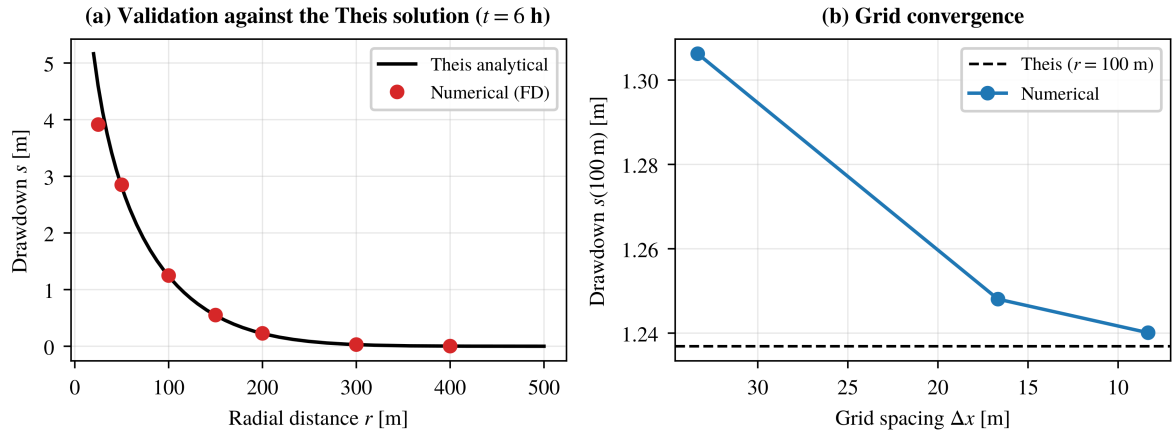


Figure 4. Verification and validation: (a) computed transient drawdown (points) against the Theis analytical solution (line) at $t = 6$ h for a single well in a homogeneous confined aquifer; (b) grid convergence of the drawdown at $r = 100$ m toward the analytical value as $\Delta x \to 0$.

Declarations

Author Contributions: Conceptualization, R.K.; methodology, B.M.; software, B.M.; validation, R.K.; investigation, D.H.; visualization, D.H.; writing—original draft preparation, B.M.; writing—review and editing, R.K. All authors have read and agreed to the published version of the manuscript.

Funding: This research received no specific grant from any funding agency in the public, commercial, or not-for-profit sectors.

Ethics Approval: Not applicable. This is a mathematical and numerical study involving no human or animal subjects.

Informed Consent and Consent for Publication: Not applicable. The submitted study reports no human participants or identifiable personal data.

Data Availability Statement: The finite-difference solver and the data underlying the figures and verification/validation tests are available from the corresponding author on reasonable request.

Acknowledgments: The submitted manuscript does not specify acknowledgments. The authors should confirm whether any acknowledgments are needed before publication.

Conflicts of Interest: The authors declare no conflict of interest.

Artificial Intelligence Disclosure: An AI assistant was used for technical formatting and LaTeX typesetting of the submitted manuscript. The authors should review and approve this statement and declare any additional AI use, if applicable. No use of AI in the underlying scientific research is asserted.

Nomenclature and Abbreviations

Symbol / acronym	Definition
h	Piezometric head (m)
Q_i	Well discharge (m^3/s)
p	Pore pressure (Pa)
K'/b'	Leakance (1/s)
$\mathbf{K} = \mathrm{diag}(K_x, K_y, K_z)$	Hydraulic-conductivity tensor (m/s)
α_b, C_r	Boundary and river conductance
S_s	Specific storage (1/m)
N	Surface flux (m/s)
$\mathbf{q}$	Darcy velocity (m/s)
T	Transmissivity (m^2/s)
W	Volumetric source/sink (1/s)
S	Storativity
α, n, β	Skeleton compressibility, porosity and water compressibility
$\Delta x, \Delta y, \Delta z, \Delta t$	Spatial and time steps
x, y, z	Coordinates (m)
η	Numerical time-step safety factor
t	Time (s)
$W(u)$	Theis well function
MPFA	Multi-point flux approximation

Symbol / acronym	Definition
GFDM	Generalized finite-difference method
PINN	Physics-informed neural network
CFL	Courant–Friedrichs–Lewy stability condition

References

[1] Lu C, Xu Z, Yang J, et al. An improved numerical model for groundwater flow simulation with MPFA method on arbitrary polygon grids. J Hydrol. 2022;606:127425. https://doi.org/10.1016/j.jhydrol.2021.127425.

[2] Mohtashami A, Akbarpour A, Mollazadeh M. Development of a hybrid meshless local Petrov–Galerkin and particle filter model for unconfined aquifer simulation. Groundwater. 2022;60(3):375–388. https://doi.org/10.1111/gwat.13161.

[3] Swathi B, Eldho TI. Generalized finite difference method for free surface flow modeling in unconfined aquifers. Eng Anal Bound Elem. 2024;158:214–229. https://doi.org/10.1016/j.enganabound.2023.10.024.

[4] Bianchi M, Scheidegger J, Hughes A, et al. Simulation of national-scale groundwater dynamics in geologically complex aquifer systems: an example from Great Britain. Hydrol Sci J. 2024;69(5):572–591. https://doi.org/10.1080/02626667.2024.2320847.

[5] Secci D, Godoy VA, Gómez-Hernández JJ. Physics-informed neural networks for solving transient unconfined groundwater flow. Comput Geosci. 2024;182:105494. https://doi.org/10.1016/j.cageo.2023.105494.

[6] Alakayleh Z, Fang X, Clement TP. A comprehensive performance evaluation of physics-informed neural networks for groundwater flow modeling. Groundwater. 2024;62(2):177–192.

[7] Dai H, Chen X, Ye M, et al. Deep learning in groundwater modeling: methods, applications and challenges. J Hydrol. 2025;650:132456.

[8] Wang N, Chang H, Zhang D. Data-driven methods for flow and transport in porous media: a review. Int J Heat Mass Transf. 2024;235:126149.

[9] Gotovac H, Malenica L, Gotovac B. Control volume isogeometric analysis for groundwater flow modeling in heterogeneous porous media. Adv Water Resour. 2021;148:103838. https://doi.org/10.1016/j.advwatres.2020.103838.

[10] Chakraborty A, Rabinovich A, Chaudhuri A. Reduced-order modeling of groundwater flow in heterogeneous porous media. J Comput Phys. 2020;412:109426.

[11] Ravshanov N, Aminov S, Shafiev T. Mathematical modeling of fluid filtration in porous media: numerical algorithms and software. Int J Appl Math. 2024;37(2):145–162.

[12] Khuzhayorov B, Usmonov A, Nik Long NMA, et al. Anomalous solute transport in a two-zone heterogeneous porous medium. Appl Math Model. 2023;124:1–18.

[13] Kresic N, Mikszewski A. Recent developments and trends in groundwater flow and transport modeling. Hydrogeol J. 2023;31:1249–1271.

[14] Darcy H. Les Fontaines Publiques de la Ville de Dijon. Victor Dalmont; 1856.

[15] Theis CV. The relation between the lowering of the piezometric surface and the rate and duration of discharge of a well using groundwater storage. Trans Am Geophys Union. 1935;16(2):519–524.

[16] Bear J, Cheng AHD. Modeling Groundwater Flow and Contaminant Transport. Springer; 2010.

[17] de Marsily G. Quantitative Hydrogeology: Groundwater Hydrology for Engineers. Academic Press; 1986.

[18] Patankar SV. Numerical Heat Transfer and Fluid Flow. Hemisphere Publishing; 1980.

[19] Peaceman DW. Interpretation of well-block pressures in numerical reservoir simulation. Soc Pet Eng J. 1978;18(3):183–194.

[20] Hantush MS, Jacob CE. Non-steady radial flow in an infinite leaky aquifer. Trans Am Geophys Union. 1955;36(1):95–100.

[21] von Neumann J, Richtmyer RD. A method for the numerical calculation of hydrodynamic shocks. J Appl Phys. 1950;21(3):232–237.

[22] Lax PD, Richtmyer RD. Survey of the stability of linear finite difference equations. Commun Pure Appl Math. 1956;9(2):267–293.

Disclaimer of Liability/Publisher's Note

The statements, opinions, and data contained in all publications are solely those of the individual author(s) and contributor(s) and do not necessarily reflect the views of the Publisher, the Journal, or the editors. The Publisher, the Journal, and the editors disclaim responsibility for any injury to persons or damage to property resulting from any ideas, methods, instructions, or products referred to in the content.